

Figure 1. (A) Schematic representation of the genome organization of MAB_2299c and its two adjacent the *mmpS-mmpL* couples (MAB_2300-MAB_2301 and MAB_2302-MAB_2303) in *M. abscessus*. The sizes and positions of the two intergenic regions (IR_{2300/01} and IR_{2302/03}) are indicated. **(B)** Transcriptional expression of the MAB_2300-MAB_2303 genes in the parental *M. abscessus* strain and in 6 spontaneous mutants selected for resistance to CFZ and harbouring mutations in MAB_2299c. Results are expressed as fold induction levels in the mutants strains relative to the parental strain. Error bars indicate standard deviation. Relative gene expression was calculated using the 2- $\Delta\Delta C_t$ method with E correction. Data is representative of three independent experiments.

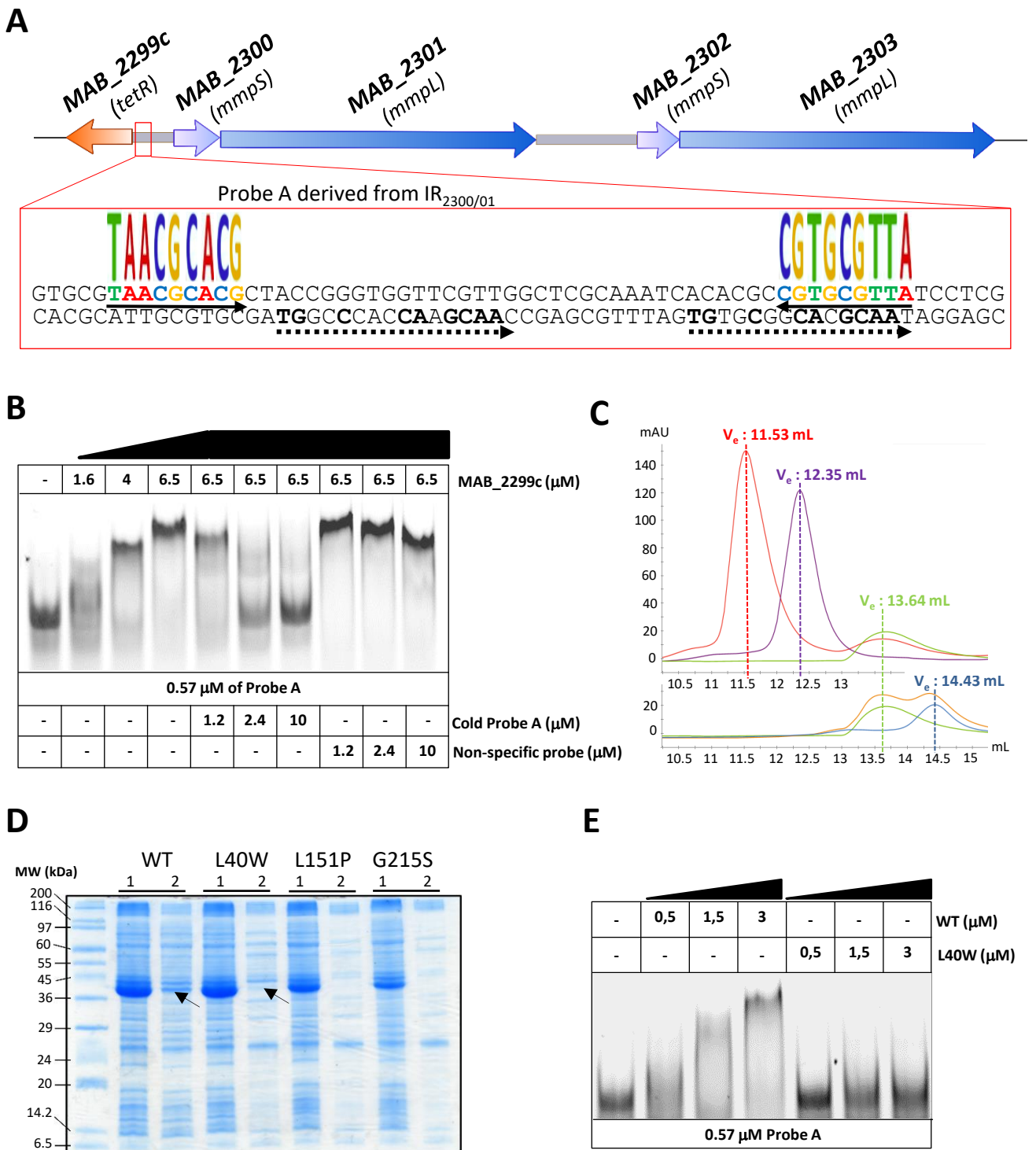
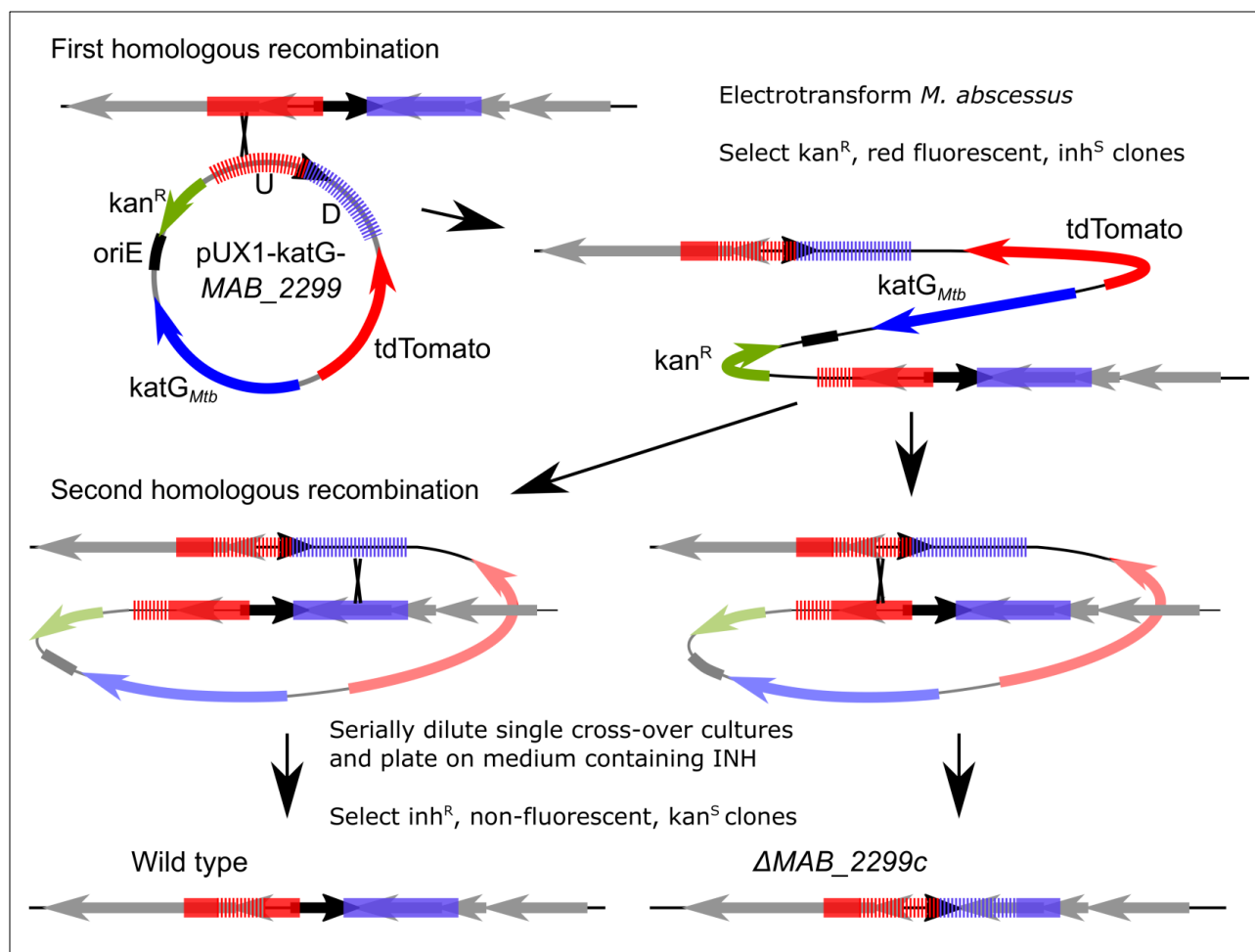


Figure 2. Binding activity of MAB_2299c to the intergenic region upstream of MAB_2300/MAB_2301. (A) Schematic representation of the 64 bp DNA operator identified within IR_{2300/01} corresponding to Probe A. The oligonucleotides recognized by MAB_2299c is composed of two degenerated palindromes and two degenerated double repeats (underlined by dashed arrows). (B) EMSA and competition assays using the Probe A and purified MAB_2299c. Gel Shifts were revealed by fluorescence emission using a 5' fluorescein-labeled Probe A. (C) Gel filtration Profiles of the free Probe A, free MAB_2299c and the TetR:DNA complex. Probe A (purple line) and MAB_2299c (green line) were isolated individually by size exclusion chromatography, displaying elution volumes of 12.35 mL and 13.64 mL respectively. When mixed together, a stable MAB_2299c:Probe A complex (red line) was also observed with an elution volume of 11.53 mL. The DNA target of the TetR regulator MAB_4384 (blue line) was elutes with 14.43 mL. However, when mixed together with MAB_2299c no protein/DNA complex was formed and both the DNA and protein were eluted separately (orange line). (D) Expression of the various MAB_2299c variants in *E. coli*. Lane 1: total crude extract; lane 2: clarified/soluble extract. The theoretical molecular mass of MAB_2299c-6His-TrxA is 41 420 Da. (E) Impaired DNA-binding activity of MAB_2299c L40W mutant as shown by EMSA using either soluble MAB_2299c (WT) or MAB_2299c (L40W) proteins. Gel Shifts were revealed by fluorescence emission thanks to the fluorescein-labeled Probe A.

A



B

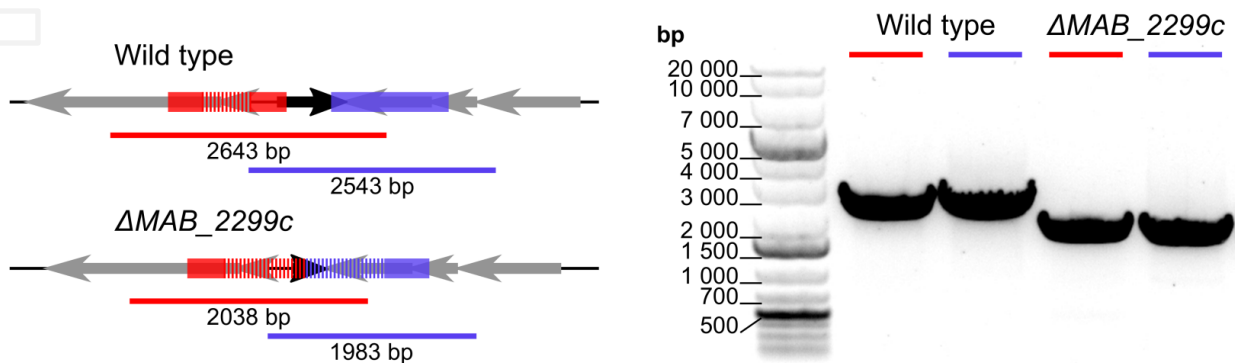


Figure 3. Generation of an unmarked *MAB_2299* deletion mutant in *M. abscessus*. (A) Line drawing illustrating the general protocol followed to ascertain the ΔMAB_2299 mutant. (B) Line drawing (left) of the chromosome context in Wt *M. abscessus* and in the ΔMAB_2299 mutant, also illustrating the PCR strategy followed to confirm deletion of *MAB_2299*. The red and blue bars indicate the PCR products obtained during the screening of potential mutant clones. A gel (right) confirming the ΔMAB_2299 genotype. The red and blue bars correspond to the amplicons obtained in the left panel.

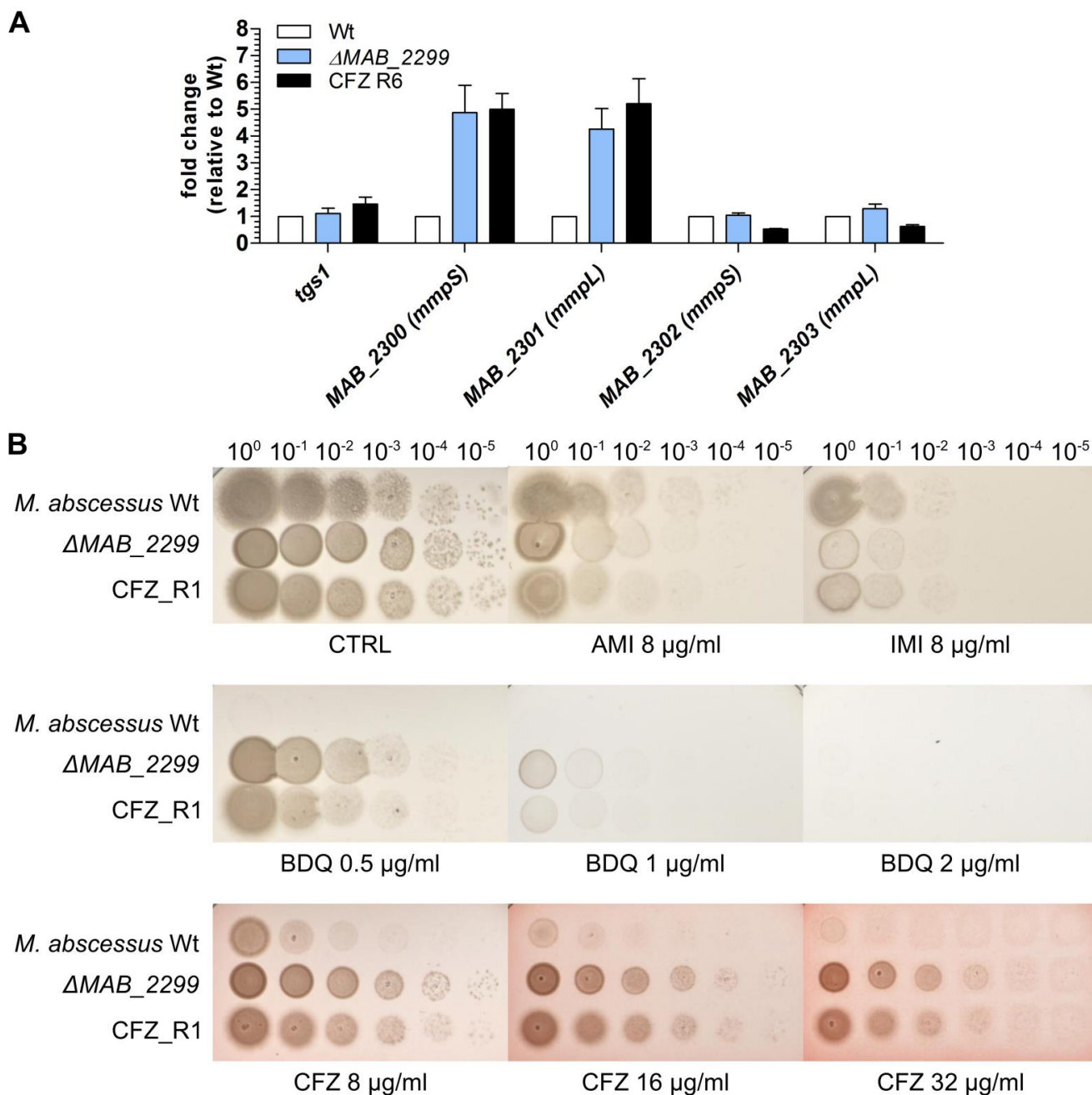


Figure 4. An unmarked deletion mutant of *MAB_2299* is resistant to clofazimine and bedaquiline. (A) qRT-PCR experiment showing induction of the *mmpS-mmpL* couple, *MAB_2300-MAB_2301*, but not *MAB_2302-MAB_2303*, when *MAB_2299* is deleted from the *M. abscessus* genome. (B) Resistance to bedaquiline and clofazimine, but not to amikacin or imipenem, exhibited by the ΔMAB_{2299} mutant.

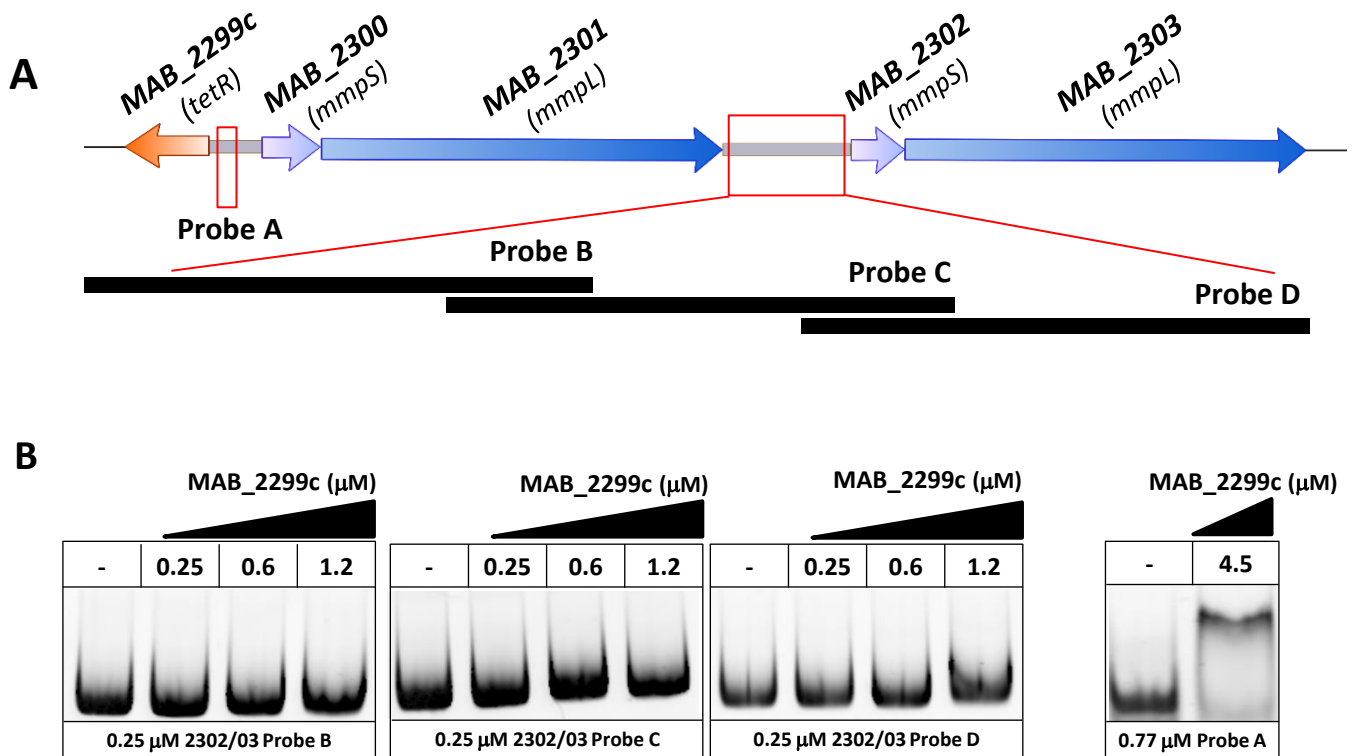


Fig. S1. (A) Schematic representation of the intergenic regions $\text{IR}_{2302/03}$ present upstream of *MAB_2302*/*MAB_2303*. Due to its size, this 893 bp region was divided in three 373 bp overlapping probes (Probes B – C – D). **(B)** EMSA using purified increasing concentrations of MAB_2299c with Probe A (left panel), Probe B (middle panel) or Probe C (right panel). Probe A was also included as a positive control (far right panel). Gel Shifts were revealed by fluorescence emission using 5' fluorescein-labeled probes. Experiments were repeated three times with similar results.